

Anomalous Coexistence of Ferroelectric Phases ($P \parallel a$ and $P \parallel c$) in Orthorhombic $\text{Eu}_{1-y}\text{Y}_y\text{MnO}_3$ ($y > 0.5$) Crystals

Mitsuru AKAKI*, Masaaki HITOMI, Mizuaki EHARA, ¹Daisuke AKAHOSHI, and
Hideki KUWAHARA

Department of Physics, Sophia University, Tokyo 102-8554, Japan

¹ *Department of Physics, Toho University, Funabashi 274-8510, Japan*

We have investigated the magnetic and dielectric properties of orthorhombic $\text{Eu}_{1-y}\text{Y}_y\text{MnO}_3$ ($0 \leq y \leq 0.6$) single crystals without the presence of the $4f$ magnetic moments of the rare-earth ions. In $y \geq 0.2$, the magnetic-structure driven ferroelectricity is observed. The ferroelectric transition temperature is steeply reducing with increasing y . In $y \geq 0.52$, two ferroelectric phases ($P \parallel a$ and $P \parallel c$) are coexistent at low temperatures. In these phases, ferroelectricity has different origin, which is evidenced by the distinctive poling-electric-field dependence of electric polarization. Namely, the electric polarization along the c axis (P_c) is easily saturated by a poling electric field, therefore P_c is caused by the bc spiral antiferromagnetic order. On the other hand, the electric polarization along the a axis (P_a) is probably attributed to the collinear E -type antiferromagnetic order, because P_a is unsaturated even in a poling field of 10^6 V/m.

KEYWORDS: multiferroic, magnetoelectric property, perovskite manganese oxide, phase diagram

*E-mail: m-akaki@sophia.ac.jp

The observation of ferroelectricity accompanied by a magnetic order in TbMnO_3 has led to a renewed interest in research on magnetoelectric multiferroics.¹ RMnO_3 (R : rare earth) with an orthorhombic perovskite structure is one of the most typical examples of the recently-discovered multiferroic materials. In $R = \text{La} - \text{Eu}$, RMnO_3 has a collinear A -type antiferromagnetic (AFM) ground state of Mn $3d$ spins. With decreasing the R -site ionic radius, the magnetic ground state changes from the A -type AFM order to a non-collinear transverse spiral AFM one around $R = \text{Gd}$, owing to the magnetic frustration between the nearest neighbor (NN) ferromagnetic and the next NN AFM interactions among Mn spins.^{2,3} In RMnO_3 ($R = \text{Tb}, \text{Dy}$), the noncollinear transverse spiral AFM order breaks the inversion symmetry through the inverse Dzyaloshinskii–Moriya (DM) interaction, resulting in the appearance of ferroelectricity.^{4–7} In other words, in the transverse spiral spin structure, the spin chirality can induce the electric polarization $\mathbf{P} \propto \sum_{ij} \mathbf{e}_{ij} \times (\mathbf{S}_i \times \mathbf{S}_j)$ in terms of the spin current mechanism, where \mathbf{e}_{ij} denotes the unit vector connecting the interacting neighbor spins \mathbf{S}_i and \mathbf{S}_j . The spin helicity or vector spin chirality of the spiral spin structure can be changed by external magnetic fields, and then the direction of the ferroelectric polarization due to the spin chirality can also be controlled by the fields.⁸ With further decreasing the R -site ionic radius from Dy, the ground state changes from the noncollinear spiral AFM order to a collinear E -type AFM one ($R = \text{Ho} - \text{Lu}$, and Y). RMnO_3 with the E -type AFM order also exhibits ferroelectric behavior, which is caused not by the inverse DM interaction but by the inverse Goodenough–Kanamori (GK) interaction, that is, the symmetric exchange striction term expressed as $\mathbf{S}_i \cdot \mathbf{S}_j$.^{9–11} This type of ferroelectricity is also realized in DyFeO_3 ¹² and $\text{Ca}_3(\text{Co}, \text{Mn})_2\text{O}_6$.¹³

The magnetoelectricity of RMnO_3 is largely affected not only by the magnetic frustration of Mn $3d$ spins but also by $4f$ magnetic moments of R^{3+} . A part of the results on $\text{Eu}_{1-y}\text{Y}_y\text{MnO}_3$ that excludes the influence of $4f$ moments by using Eu^{3+} ($J = 0$) and Y^{3+} (nonmagnetic) has been reported in our preceding paper.¹⁴ Furthermore, details of the effect of $4f$ moments were clarified from the comparative study of $(\text{Eu}, \text{Y})_{1-y}\text{Tb}_y\text{MnO}_3$ and $(\text{Eu}, \text{Y})_{1-y}\text{Gd}_y\text{MnO}_3$ crystals with different $4f$ magnetic characters.¹⁵ The results of our experiments clearly show that the ferroelectricity of RMnO_3 is greatly influenced by the existence of a small amount of $4f$ moment. Therefore, in this study, we focused on $4f$ -moment-free system $\text{Eu}_{1-y}\text{Y}_y\text{MnO}_3$. The ground state of

$\text{Eu}_{1-y}\text{Y}_y\text{MnO}_3$ changes from a canted *A*-type AFM and paraelectric phase with concentration $y < 0.15$ toward a presumably spiral AFM and ferroelectric one with $y \geq 0.3$ (see also Fig. 4).^{16,17} In the case of $y = 0.405$ for $\text{Eu}_{1-y}\text{Y}_y\text{MnO}_3$, the direction of the ferroelectric polarization spontaneously changes from along the *c*-axis (P_c) at higher temperatures to the *a*-axis (P_a) at lower temperatures in a zero magnetic field.¹⁴ In the ferroelectric phase of $y = 0.405$, the spiral spin structure is confirmed by neutron scattering measurements.¹⁸ However, P_c is a minor phase and its magnitude is much smaller than that of P_a in the $y = 0.405$ sample. To clarify the phase competition between the P_a and the P_c states, it is necessary to develop the P_c phase and to enhance its magnitude by increasing y . This is because the P_c region expands with increasing Y concentration y as shown in Fig. 4. In addition, with increasing y or equivalently decreasing the average ionic radius of *R* site, the emergence of the ferroelectric state with the *E*-type AFM order is believed to occur, as observed in polycrystalline form.¹¹ In this study, to reveal the electronic phase separation or coexistence between the P_a and the P_c phases as well as to achieve the ferroelectric phase with the *E*-type AFM order, we have investigated the magnetic and ferroelectric properties of orthorhombic $\text{Eu}_{1-y}\text{Y}_y\text{MnO}_3$ (especially for $y > 0.5$) single crystals, in which development of the P_c phase and the emergence of *E*-type AFM order are expected.

2. Experiment

We prepared a series of $\text{Eu}_{1-y}\text{Y}_y\text{MnO}_3$ ($0 \leq y \leq 0.6$) single crystals which were grown by a floating zone method. In order to stabilize the orthorhombic phase, we used high-pressure oxygen of 7.5 atm as a growth atmosphere for $0.5 \leq y \leq 0.6$ crystals, while argon of 2.5 atm for $0 \leq y < 0.5$ crystals. We performed X-ray diffraction (XRD) measurements on the obtained crystals at room temperature. The Rietveld analysis of powder XRD data revealed that all the samples have an orthorhombic $Pbnm$ structure without a hexagonal impurity phase or any phase segregation. All the single crystalline samples used in this study were cut along the crystallographic principal axes into a platelike shape using an X-ray back-reflection Laue technique. We also prepared the sample oriented along the $[101]$ direction to investigate the phase coexistence of P_a and P_c . The dielectric constant and the ferroelectric polarization were measured using a temperature-controllable cryostat. The dielectric constant measurement was performed with an *LCR* meter at a frequency of 10 kHz (Agilent, 4284A). The pyroelectric current to obtain the spontaneous electric polarization was measured in a warming process at

a rate of 4 K/min after the samples were cooled from 60 to 5 K in a poling electric field of 20 ~ 1020 kV/m. The magnetic properties and specific heat were measured using a commercial apparatus (Quantum Design, PPMS-9T).

3. Results and discussion

Let us start with the results of $\text{Eu}_{0.45}\text{Y}_{0.55}\text{MnO}_3$. Figure 1 shows the temperature dependence of (a) dielectric constant, (b) electric polarization, (c) magnetization, and (d) specific heat divided by temperature C/T . The sample shows the anisotropic magnetization below 45 K, above which a common paramagnetic behavior is observed along all axes. Below 45 K, the magnetization parallel to the b -axis (M_b) steeply decreases whereas that along the a (M_a)- and c (M_c)- axes remains almost constant in the temperature range from 45 down to 18 K. This result implies that the AFM order has a magnetic easy axis parallel to the b -axis. P_c rises up sharply below 18 K, where the dielectric constant along the c -axis (ε_c) shows a small peak concomitantly. The slight anomaly is observed also in the M_c and C/T around the same ferroelectric transition temperature. On the other hand, the P_a phase develops gradually below 18 K, where ε_a shows a faint anomaly. A broad peak of ε_a is observed around 10 K, below which coexistence of the P_a and the P_c phases is prominent. To ensure that this coexistence is not an experimental artifact such as misalignment of the sample direction, we have measured the ferroelectric polarization along the [101] direction (Fig. 1 (b)). Then, we have observed the distinctive feature of P_{101} , which is consistent with the expected $(P_a + P_c)$ value projected on to the [101] direction. This is in sharp contrast to the case of the $y = 0.405$ sample, in which the emergence of the P_a phase and the disappearance of the P_c phase occurred simultaneously at a certain temperature.¹⁴ In other words, the temperature-induced electric polarization flop, i.e., 90°-rotation of the polarization, was observed. Therefore, there is no indication of coexistence of both the P_a and the P_c phases in the $y = 0.405$ sample.

Figure 2 shows the temperature dependence of P_a and P_c of $\text{Eu}_{0.45}\text{Y}_{0.55}\text{MnO}_3$ in various poling electric fields. P_c is saturated at a field of 110 kV/m with a value of about 230 $\mu\text{C}/\text{m}^2$. On the other hand, P_a is not saturated even in a field of 1020 kV/m. P_a can possibly indicate a larger magnitude in a stronger poling field. The observed large difference in saturation electric fields of the P_a and the P_c phases suggests that each phase has a different origin of its ferroelectricity. Namely, the P_c phase originates from the inverse DM interaction for the bc -spiral spin structure. A saturation poling

field of about 100 kV/m for the P_c phase is comparable to those for other ferroelectric phases due to the inverse DM interaction. On the other hand, the P_a phase seems to arise from the inverse GK interaction for the E -type AFM order which is expected to exist in such high- y samples.²⁰ The similar poling field dependence of P_a , that is, no saturation of P_a up to 500 kV/m, is reported in a polycrystalline YMnO_3 sample in which the E -type AFM order is confirmed by neutron scattering.¹⁰

Therefore, the data shown in Figs. 1 and 2 clearly evidence that the P_a and the P_c phases with different origins coexist in low temperatures especially below 10 K. These results indicate that this coexisting state originates from the difference of the AFM orders that cause P_a or P_c . In the $y = 0.60$ sample, a similar poling field dependence to that of $y = 0.55$ was observed.

Figure 3 (a) shows the temperature dependence of P_a and P_c of $y = 0.52$ located near the phase boundary. The P_a and the P_c phases of $y = 0.52$ show a similar behavior to $y = 0.55$ (see also Fig. 1 (b)); therefore, we conclude that the P_a phase of $y = 0.52$ is also induced by the E -type AFM order. However, in contrast to the $y = 0.55$, P_c is strongly suppressed and slightly decreases below 10 K where P_a sharply rises up. This polarization-flop-like behavior is widely observed in the (magnetic-field-induced) phase transition from the bc -spiral AFM (P_c) state to the ab -spiral (P_a) one, as discussed above for the $y = 0.405$ sample. These results suggest also that the P_a phase of $y = 0.52$ is not almost due to the ab -spiral AFM order but mainly due to the E -type AFM one. The ferroelectric polarization along the a -axis of $y = 0.405$, 0.52, and 0.55 at 5 K as a function of the poling electric field is shown in Fig. 3 (b). In $y = 0.405$, P_a is easily saturated in a low poling field (about 100 kV/m) as well as P_c of $y = 0.55$ (Fig. 2 (b) inset). On the other hand, the saturation poling field of P_a of $y = 0.52$ is about 700 kV/m. The increase of saturation poling field is due to the increase of the E -type AFM nuclei embedded in the spiral AFM phase by increasing Y concentration y . It is reasonable that a small amount of the ab -spiral AFM phase remains in the E -type AFM one at low temperatures, because $y = 0.52$ is located near the phase boundary (see Fig. 4).

We have summarized the obtained data into a magnetoelectric phase diagram for $\text{Eu}_{1-y}\text{Y}_y\text{MnO}_3$ crystals with $0 \leq y \leq 0.6$ (Fig. 4). The ferroelectric transition temperature is steeply reducing with increasing y . In $y > 0.5$, the P_c region drastically expands compared with that of $y = 0.405$. As already discussed, in the $y = 0.405$ sample,¹⁴

P_c emerges below 25 K and disappears at 23 K, below which P_a is observed. That is, the ferroelectric polarization flops from the c -axis to the a -axis at 23 K. This polarization flop is assigned to the orthogonal flop of the spin spiral plane from the bc (P_c) to the ab (P_a). It should be noted that P_c and P_a are coexistent at low temperatures in $0.52 \leq y \leq 0.6$ (right hatched area in Fig. 4). The P_a phase in the coexisting state should be attributed not to the ab -spiral AFM spin order but to the E -type AFM one. Because P_c is easily saturated at a poling field of ~ 100 kV/m, it is caused by the bc -spiral AFM order. On the other hand, P_a is probably caused by the collinear E -type AFM order, because the poling electric field dependence of P_a in $0.52 \leq y \leq 0.6$ as shown in Fig. 2 (b), is very similar to that of P_a due to the E -type AFM order in a polycrystalline form.¹⁰ However, the presence of the ab -spiral AFM (P_a) phase cannot be ruled out as a possible source of P_a . To confirm the appearance of the E -type AFM phase more directly, synchrotron X-ray and/or neutron diffraction measurements are required.

4. Conclusion

We have investigated the magnetic and dielectric properties of orthorhombic $\text{Eu}_{1-y}\text{Y}_y\text{MnO}_3$ ($0 \leq y \leq 0.6$) single crystals without the presence of the $4f$ magnetic moments of the rear-earth ions. In $y \geq 0.52$, two ferroelectric phases ($P \parallel a$ and $P \parallel c$) are coexistence at low temperatures. P_c is induced by the noncollinear transverse spiral spin structure. On the other hand, P_a is likely induced by the collinear E -type AFM order through the symmetric exchange striction term. The two-phase coexisting state ($P_a + P_c$) would provide a novel route toward the control of dielectric (magnetic) properties by magnetic (electric) fields.

Acknowledgment

This work was partly supported by Grant-in-Aid for JSPS Fellows from Japan Society for Promotion of Science.

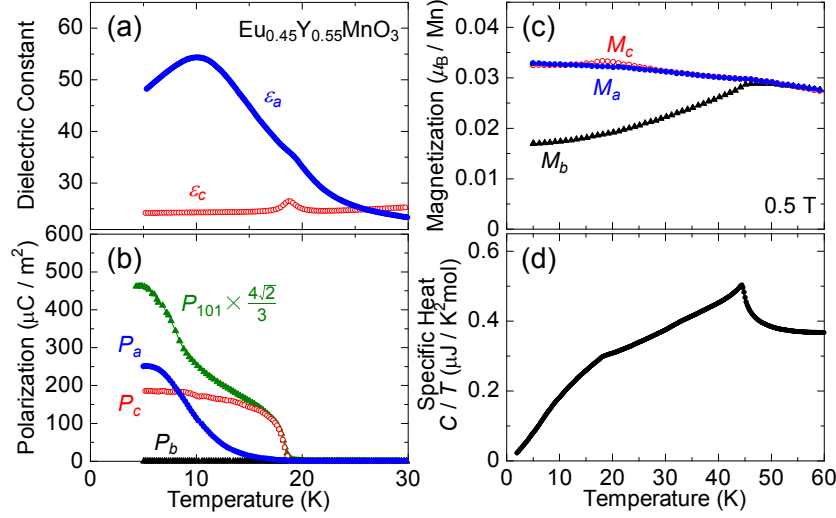


Fig. 1. (Color online) Temperature dependence of (a) dielectric constant along the a - and c -axes, (b) electric polarization along the a , b , c , and $[101]$ directions, (c) magnetization along the each principal axis, and (d) specific heat divided by temperature of $\text{Eu}_{0.45}\text{Y}_{0.55}\text{MnO}_3$. To compare the $(P_a + P_c)$ value, P_{101} is multiplied by a factor of $\frac{4\sqrt{2}}{3}$.¹⁹ The magnetization was measured in 0.5 T.

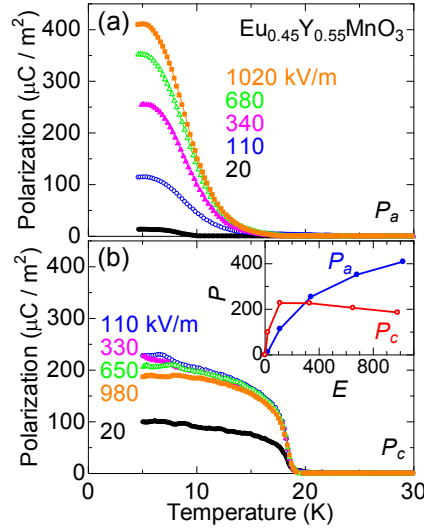


Fig. 2. (Color online) Temperature dependence of ferroelectric polarization along (a) the a -axis and (b) the c -axis of $\text{Eu}_{0.45}\text{Y}_{0.55}\text{MnO}_3$ crystal in various poling electric fields, which were applied in the cooling process and removed before the measurements of polarization. The inset shows the value of ferroelectric polarization along the a - and c -axes at 5 K as a function of the poling electric field.

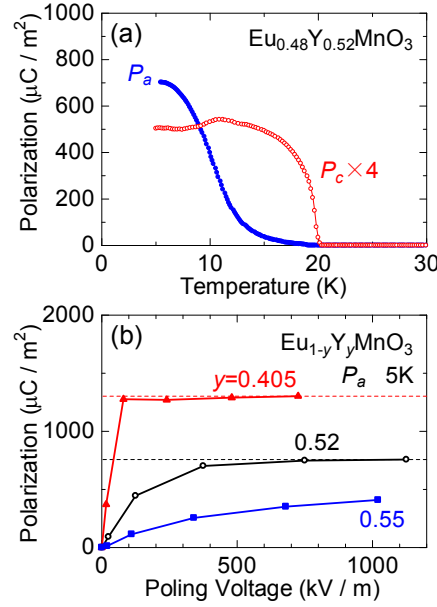


Fig. 3. (Color online) (a) Temperature dependence of ferroelectric polarization along the a - and c -axes of $y = 0.52$. P_c is multiplied by a factor of 4 for comparison. (b) The value of ferroelectric polarization along the a -axis of $y = 0.405$, 0.52 , and 0.55 at 5 K as a function of the poling electric field. The dotted lines are guides to the eye.

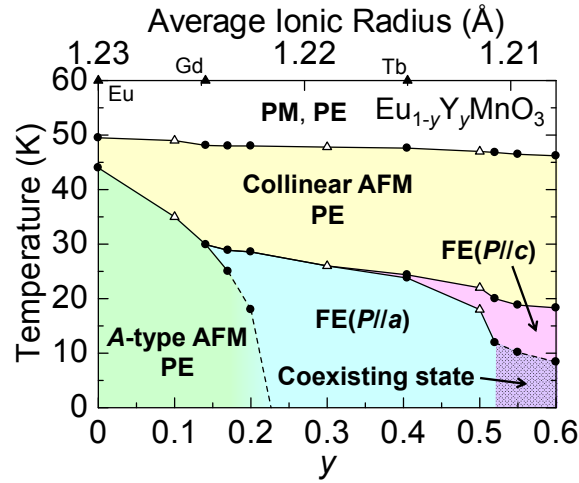


Fig. 4. (Color online) The magnetoelectric phase diagram of $\text{Eu}_{1-y}\text{Y}_y\text{MnO}_3$ with $0 \leq y \leq 0.6$. The abbreviations mean paramagnetic (PM), paraelectric (PE), antiferromagnetic (AFM), and ferroelectric (FE) phases. The data points are obtained from the measurements of the dielectric constant, and from Ref. 16 (Δ). The hatched area in the right bottom region means the phase-coexisting state. The upper horizontal axis indicates the average ionic radius of $(\text{Eu}_{1-y}\text{Y}_y)$ ion, which corresponds to the y value in lower axis. Solid triangles in upper axis denote the ionic radius of each rare earth ion.

References

- 1) T. Kimura, T. Goto, H. Shintani, K. Ishizaka, T. Arima, and Y. Tokura: *Nature* **426** (2003) 55.
- 2) T. Kimura, S. Ishihara, H. Shintani, T. Arima, K. T. Takahashi, K. Ishizaka, and Y. Tokura: *Phys. Rev. B* **68** (2003) 060403(R).
- 3) T. Goto, T. Kimura, G. Lawes, A. P. Ramirez, and Y. Tokura: *Phys. Rev. Lett.* **92** (2004) 257201.
- 4) H. Katsura, N. Nagaosa, and A. V. Balatsky: *Phys. Rev. Lett.* **95** (2005) 057205.
- 5) M. Mostovoy: *Phys. Rev. Lett.* **96** (2006) 067601.
- 6) M. Kenzelmann, A. B. Harris, S. Jonas, C. Broholm, J. Schefer, S. B. Kim, C. L. Zhang, S.-W. Cheong, O. P. Vajk, and J. W. Lynn: *Phys. Rev. Lett.* **95** (2005) 087206.
- 7) T. Arima, A. Tokunaga, T. Goto, H. Kimura, Y. Noda, and Y. Tokura: *Phys. Rev. Lett.* **96** (2006) 097202.
- 8) Y. Yamasaki, H. Sagayama, T. Goto, M. Matsuura, K. Hirota, T. Arima, and Y. Tokura: *Phys. Rev. Lett.* **98** (2007) 147204.
- 9) I. A. Sergienko, C. Sen, and E. Dagotto: *Phys. Rev. Lett.* **97** (2006) 227204.
- 10) B. Lorenz, Y. Q. Wang, and C. W. Chu: *Phys. Rev. B* **76** (2007) 104405.
- 11) S. Ishiwata, Y. Kaneko, Y. Tokunaga, Y. Taguchi, T. Arima, and Y. Tokura: *Phys. Rev. B* **81** (2010) 100411(R).
- 12) Y. Tokunaga, S. Iguchi, T. Arima, and Y. Tokura: *Phys. Rev. Lett.* **101** (2008) 097205.
- 13) Y. J. Choi, H. T. Yi, S. Lee, Q. Huang, V. Kiryukhin, and S.-W. Cheong: *Phys. Rev. Lett.* **100** (2008) 047601.
- 14) K. Noda, M. Akaki, T. Kikuchi, D. Akahoshi, and H. Kuwahara: *J. Appl. Phys.* **99** (2006) 08S905.
- 15) M. Hitomi, M. Ehara, M. Akaki, D. Akahoshi, and H. Kuwahara: *J. Phys. Soc. Jpn.* **79** (2010) 054704.
- 16) J. Hemberger, F. Schrettle, A. Pimenov, P. Lunkenheimer, V. Yu. Ivanov, A. A. Mukhin, A. M. Balbashov, and A. Loidl: *Phys. Rev. B* **75** (2007) 035118.

- ~~17) Y. Yamasaki, S. Miyasaka, T. Goto, H. Sagayama, T. Arima, and Y. Tokura: Phys. Rev. B **76** (2007) 184418.~~
- 18) R. Kajimoto, T. Yokoo, M. Kofu, K. Noda, and H. Kuwahara: J. Phys. Chem. Solids **68** (2007) 2087.
- 19) From the ratio of the P_{101} to the $(P_a + P_c)$ values measured in the series of $RMnO_3$, the correction coefficient to convert the observed P_{101} value into the expected $(P_a + P_c)$ value was estimated to be $\frac{4\sqrt{2}}{3}$, which is roughly equal to the simple expectation of $\sqrt{2}$.
- 20) M. Mochizuki, N. Furukawa, and N. Nagaosa: Phys. Rev. Lett. **105** (2010) 037205.